JOURNAL OF KUFA–PHYSICS
journal.uokufa.edu.iq/index.php/jkp/index | ISSN: 2077–5830

Synthesis and Characterization of Nanostructure of Ag doped ZnO/P-Si Detectors Prepared by CBD Method

[*]Hussein Abdullah Alshamarti

Department of Physics - Faculty of Science - University of Kufa/Iraq

[*]*Corresponding Author E-mail*: husseina.alshemirti@uokufa.edu.iq

ARTICLE INF.

Article history:
Received: 4 AUG., 2025
Revised: 15 SEP., 2025
Accepted: 24 NOV., 2025
Available Online: 27 DEC. 2025

Keywords:

ZnO
Ag-doping ZnO
CBD method
detectors, nanorods.

ABSTRACT

In this work, nanostructured zinc oxide were doped with various silver doping ratios of 0%, 2%, 4%, and 8%. The nanorods were grown on silicon wafers using the chemical bath deposition (CBD) method. Aluminum contacts were evaporated onto the prepared samples using a thermal evaporation technique. Al/Ag:ZnO/Si/Al detectors were produced according to the above ratios, and were named as X1, X2, X3, and X4, respectively. The structural properties and surface morphology of the fabricated detectors were studied. The effect of (I-V) and (I-T) was also studied at a room temperature. The current values at UV wavelengths of 365 nm and 385 nm showed a distinct difference between the synthesized detectors. The photosensitivity values of the detectors based on Ag:ZnO composition (i.e. 0%, 2%, 4%, and 8%) under an applied source voltage of 5 V for samples X1, X2, X3, and X4 were 413%, 9722%, 2055% and 753% at a wavelength of 365 nm, and 444%, 4810%, 930% and 602% at a wavelength of 385 nm in UV light and a power density of 40 μW/cm², respectively. By calculating the rise and decay time for each sample and at each UV wavelength of 365 nm and 385 nm, it was found that the effect of doping was effective and good in improving and developing the prepared detectors. All detectors exhibited stability and high-speed response, especially for the extinction time.

DOI: https://doi.org/10.31257/2018/JKP/2025/v17.i02.20790

تصنيع وتوصيف لكواشف ذات التركيب النانوي لأوكسيد الزنك المشوب بالفضة /السيليكون والمحضر بطريقة ترسيب الحمام الكيميائي

حسين عبد الله الشمرتي

قسم الفيزياء – كلية العلوم – جامعة الكوفة - العراق

الـــخُـــلاصـــة

الكلمات المفتاحية:

في هذا العمل، تم تطعيم أوكسيد الزنك ذات التركيب النانوي بنسب تطعيم مختلفة بالفضة (0%، 2%، 4%، و8%). حيث تم انماء القضبان النانوية على رقائق السيليكون باستخدام طريقة الترسيب الكيميائي (CBD). وتم تبخير الألومنيوم كنقاط تلامس على العينات المُحضَّرة باستخدام تقنية التبخير الحراري.وتم تصنيع الكواشف Al/Ag:ZnO/Si/Al وفقًا للنسب التشويب المذكورة أعلاه، وتم تسميتها بX1 وX2 وX3 وX4 على التوالي. تم دراسة الخصائص الهيكلية ومورفولوجيا لسطوح الكواشف المُصنَّعة. كما تم دراسة تأثير (I-V) و(I-T) عند درجة حرارة الغرفة. حيث اظهرت قيم التيار عند أطوال موجية للأشعة فوق البنفسجية (365 نانومتر و385 نانومتر) اختلافًا واضحًا بين الكواشف المُصنَّعة. وتم حساب قيم حساسية الكواشف للضوء، بناءً على تشويب الفضةلأوكسيد الزنك (0%، 2%، 4%، و8%)، وعند تطبيق جهد مصدر قدره 5 فولت . حيث بلغت قيم العينات X1 وX2 وX3 وX4، 413% و9722% و2055% و753% عند طول موجي 365 نانومتر، و444% و4810% و930% و602% عند طول موجي 385 نانومتر في ضوء الأشعة فوق البنفسجية وكثافة طاقة 40 ميكروواط/سم²، على التوالي. وبحساب زمن الصعود والاضمحلال لكل عينة ولكل طول موجي للأشعة فوق البنفسجية 365 نانومتر و385 نانومتر، تبيّن أن تأثير التطعيم كان فعالاً وجيدًا في تحسين وتطوير الكواشف المُجهزة. وقد أظهرت جميع الكواشف ثباتًا واستجابة عالية السرعة، وخاصةً لزمن الانطفاء.

اوكسيد الزنك
تشويب الفضة لاوكسيد الزنك
طريقة ترسيب الحمام الكيميائي
الكواشف
القضبان النانوية

1. INTRODUCTION

The preparation of nanostructures in their various forms, whether rods [1], particles [2], fibers [3] .... etc, has attracted significant research interest, especially in recent years. This is due to their important role in developing and improving their structural, chemical, and physical properties. They are lead to the development and improvement of device applications and electronic components, such as solar cells [4], transistors [5], LEDs [6], gas sensors [7], and detectors [8]. Detectors and sensors are a critical component their use in diverse and essential applications. This includes flame sensing, environmental monitoring, missile plume detection, communications, medicine, etc[9]. The detectors which are based on zinc oxide nanostructures have become widely available for detecting ultraviolet radiation, which is extremely dangerous to humans[10]. The zinc oxide also possesses key physical properties that facilitate the development of these detectors, such as its wide energy gap of 3.37 eV, its safety due to its non-toxicity, its high transparency (~80-95%) in the visible spectrum, and many other unique electrical and thermal properties [11]. Studies have also shown that it is possible to control and improve the physical and chemical properties using doping approach. This is achieved by adding doping materials to the zinc oxide (ZnO) nanostructure [12], such as manganese (Mn) [13], cadmium (Cd)[14], nickel (Ni) [15], aluminum (Al) [16], and silver (Ag) [17]. The doping process contributes to improving the detector properties and enhancing the response speed, sensitivity, and electrical conductivity. There are several methods for preparing nanoscale zinc oxide, such as sol-gel method [17], pulsed laser deposition [18], hydrothermal method [19], chemical vapor deposition [20], and chemical bath deposition processes [21]. The CBD method was chosen because it does not require complex equipment and is easy to use for the preparation, doping, and growth processes on silicon wafers. Growth is

also crucial for nanorods in increasing the surface area of the detectors. Therefore, zinc oxide NRs are expected to provide a significant increase in the absorption and desorption of O2 molecules, increasing the detector efficiency.

2. Experimental details

Zinc oxide (ZnO) nanorods were deposited on a silicon substrate in several steps. In the first step, silicon wafers were washed using an ultrasonic device, propanol, acetone, and deionized water. The second step was to prepare solution of the seed layer by dissolving 0.025 mol of zinc acetate (CH3COO)2.2H2O) in absolute ethanol at 60 °C for 3 hrs with continuous stirring. At that time, the samples were then coated with a thin layer onto clean silicon wafers at 2500 rpm for 45 s at a room temperature. The samples were dried at 130 ± 5°C for approximately 15 min to remove organic residues. This process was repeated approximately 9 times. Next, the samples were heated at 450 ± 10 °C for 2 hours using an oven. The last step, nanorods of zinc oxide (ZnO) and zinc oxide doped with (0%, 2%, 4%, and 8%) silver nitrate (AgNO3) were prepared, and these samples were designated X1, X2, X3, and X4, respectively, by the Chemical Bath Deposition way. The reactant was located perpendicular in a beaker with a 0.04 M aqueous solution of (Zn(NO3))2.6H2O and 0.04 M (C6H12N4). Furthermore, a homogeneous solution of zinc oxide doped with silver with different concentrations of 0%, 2%, 4%, and 8% silver nitrate (AgNO3) was added to the reaction bath .All samples were placed in a beaker at 90 °C ± 5°C for 90 minutes. Finally, the prepared thin films were cleaned and heated at 450°C for 1 hour. Aluminum probes were placed on all prepared samples X1, X2, X3, and X4 using the thermal evaporation technique. The active area of the Al/Ag:ZO/Si/Al structure detectors were about 1 cm².

3. Results and discussion

Field-emission scanning electron microscopy (FESEM) and X-ray diffraction (XRD) were used to characterize the surface morphology and structural properties of the prepared samples, as shown in Fig.1 and Fig.2, respectively.

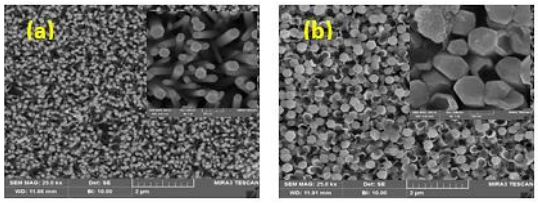

Fig.1: image (FESEM) of the samples prepared a) X1, b) X3

The FESEM images of the prepared samples X1 and X3 clearly show a vertical array of ZnO nanorods grown on a silicon wafer. They are arranged in a uniform manner, with hexagonal wurtzite. From the Fig.1a, the average diameter of the nanorods of sample 1 ranges from 70-80 nm. The silver doping has a significant impact on the surface structure of the ZnO. Furthermore, the diameter of most of the ZnO nanorods does not exceed 90 nm as shown in the inset of Fig.1b. The slight change in shape and size of zinc oxide nanorods upon doping may

contribute to the enhanced response to UV light.

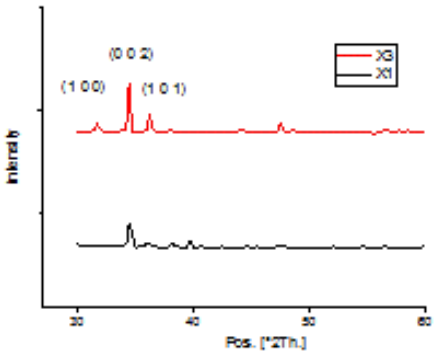

Fig.2: XRD pattern of the samples X1 & X3

The XRD patterns of the fabricate samples X1 and X3 confirm the structural and hexagonal structure of zinc oxide. Sample X1 exhibits sharp and strong peaks at (1 0 0), (0 0 2), and (1 0 1) levels, with peaks at $2\theta = 31.68^{\circ}$, $2\theta = 34.33^{\circ}$, and $2\theta = 36.09^{\circ}$, respectively. No new peaks were observed in the XRD pattern of the silver-doped sample X3. This may be due to the incorporation of silver ions into the ZnO array, which explains why there were no changes in the hexagonal wurtzite phase of the ZnO NRs. However, there was a slight shift in the peak positions, which may be due to the slight difference in the size of the doped material (silver) compared to the base material (zinc oxide). All of the obtained results are in complete agreement with previous studies [22-24].

4. Characterization of the Prepared Detectors

4.1 Current -Voltage Properties (I-V)

Fig.3 shows the current-voltage (I-V) plots in the dark and under UV light at wavelengths of 365 and 385 nm for the prepared samples X1, X2, X3, and X4, with a power density of 40 μW/cm², at a room temperature. The response of the detectors to UV light was evident through the increase in current values with changing voltage. This may attributed to the generation of electron-hole couples at the UV light energy, which contributes significantly to the increase in current. The energy gap values also play a significant role in the differentiation between UV wavelengths of 365 and 385 nm.

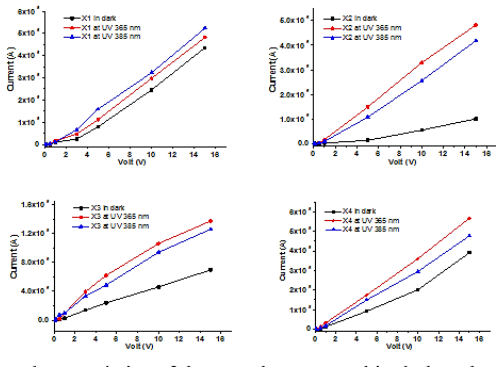

Fig. 3: I–V characteristics of the samples prepared in dark and under UV light

4.2 Current -Time (I-T) Properties

Fig. 4 shows the on/off changing properties of the prepared photodetectors at 5 Volt bias.

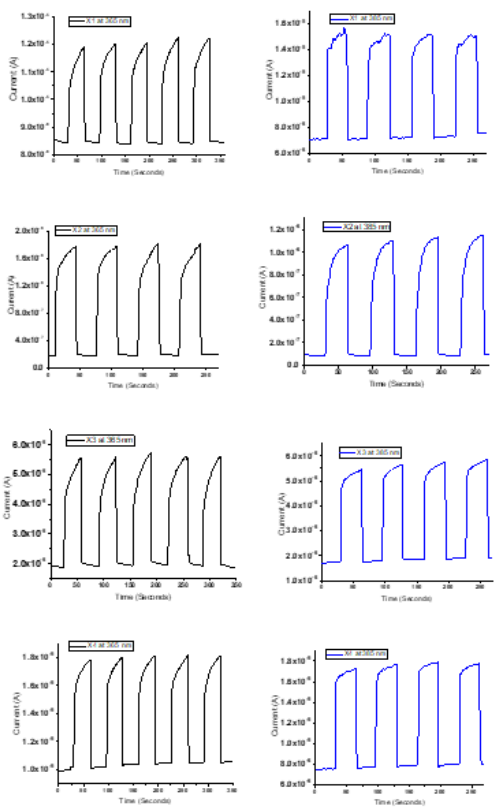

Fig. 4: photocurrent as function of time under UV light (365 & 385 nm)

The 30s/30s on/off periods were tested to determine the stability of the detectors' response at room temperature. The detectors showed good stability and high reliability, with relatively fast response and recovery times at wavelengths 365 and 385 nm of the ultra violet ray (intensity 40 μW/cm2).

4.3 Rise and Recovery Times

The adsorption of oxygen molecules and the generation of electron-hole pairs play a significant role in the detector's speed, response, and recovery time. The Fig.5 shows the rise time (Tr) and recovery time (Td) for all samples X1, X2, X3 and X4 under the influence of UV ray at a wavelength of 365 nm. Table 1 presents the rise times and recovery times for all prepared samples (X1,X2,X3 and X4) at wavelengths of 365 and 385 nm, which were calculated using the same method [25]. The results show that the Ag-doped ZnO detectors exhibited faster light response and better recovery times than the undoped zinc detector.

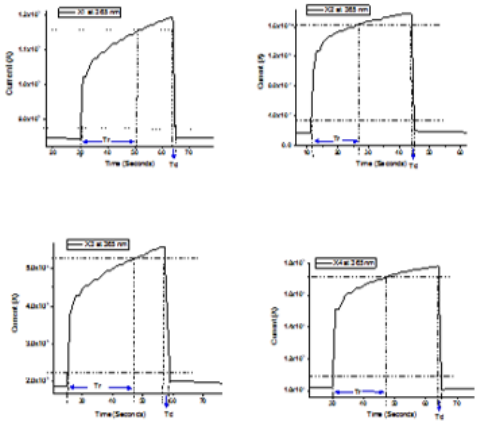

Fig. 5: The rise and decay times for all sample prepared under UV wavelengths 365 nm.

Table 1: The values of the rise and decay times for all sample

samples	Under wavelength 365 nm		Under wavelength 385 nm	
	Tr (sec)	Td (sec)	Tr (sec)	Td (sec)
X1	27	1	24	1.5
X2	15.4	0.93	14.773	1.2
X3	21.6	1.7	19.3	1.42
X4	17	0.65	16	1

4.4 Photosensitivity (S)

The comparison between the impurities and unpurified detectors for wavelengths 365 and 385 nm was done by calculating the Photosensitivity of all the prepared detectors according to the following equation[26]:

$$S = \frac{I_{ph} - I_{dark}}{I_{dark}} \times 100\% \quad (1)$$

The Ag:ZnO photodetectors (X2, X3, and X4) exhibited superior response and Photosensitivity compared to the ZnO photodetector (X1), as shown in Fig.6. These detectors could be potential candidates for a wide domain of UV sensor fabrication devices by controlling the doping ratios, shape, and nanoscale.

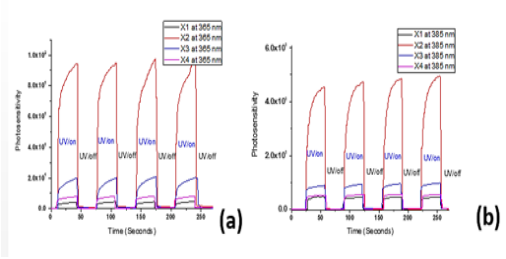

Fig. 6: Photosensitivity of the samples prepared at UV wavelength of (a) 365 nm and (b) 385 nm

5. Conclusion

A zinc oxide rod array (sample X1) and doped ZnO with different percentages of (Ag) silver (samples X2, X3 and X4), were successfully grown on silicon substrates using the CBD method. The fabricated samples were tested as ultraviolet detectors with very low light intensity. All samples showed good response at 365 and 385 nm wavelengths and at room temperature. I-T characteristics of the prepared samples were greatly stable and reliable, which may make them promising for future applications. The role of silver doping was crucial in controlling the detectors' response to UV light, which could open new horizons for the development of a wide range of detectors.

References:

[1] Alshamarti, H.A. and A.H.O. Alkhayatt, Enhancement characterization of the MSM detector based on Mn doped-ZnO NRS synthesized by microwave assisted chemical bath deposition. Materials Science in Semiconductor Processing, 2020. 114: p. 105068.

[2] Qu, B., Z. Xiao, and Y. Luo, Sustainable nanotechnology for food preservation: Synthesis, mechanisms, and applications of zinc oxide nanoparticles. Journal of Agriculture and Food Research, 2025. 19: p. 101743.

[3] Yang, Y., et al., Homogeneous and aligned ZnO nanorods@ Jute fibers for enhanced mechanical/microwave absorbing performance and thermal stability. Materials Chemistry and Physics, 2023. 295: p. 127031.

[4] Javed, A.H., et al., Effect of ZnO nanostructures on the performance of dye sensitized solar cells. Solar Energy, 2021. 230: p. 492-500.

[5] You, H.-C., et al. The transistor characteristics of zinc oxide active layer with different thickness of zinc oxide thin-film. in 2012 International Symposium on Computer, Consumer and Control. 2012. IEEE.

[6] Baek, S.-D., et al., Fabrication of ZnO homojunction-based color-switchable bidirectional LEDs by using a hydrothermal growth method. Journal of Materials Chemistry C, 2017. 5(36): p. 9479-9487.

[7] Kang, Y., et al., Review of ZnO-based nanomaterials in gas sensors. Solid State Ionics, 2021. 360: p. 115544.

[8] Aljanaby, H.A.J. and H.A. Alshamarti. Synthesis Ni-doped ZnO nanorod of UV photodetector by chemical bath deposition. in AIP Conference Proceedings. 2023. AIP Publishing LLC.

[9] Harris, C., A. Bailey, and T. Dodd, Multi-sensor data fusion in defence and aerospace. The Aeronautical Journal, 1998. 102(1015): p. 229-244.

[10] Li, Y., C. Liao, and S.C. Tjong, Recent advances in zinc oxide nanostructures with antimicrobial activities. International Journal of Molecular Sciences, 2020. 21(22): p. 8836.

[11] Nassir, L.F., A.S. Hussein, and H.H. Fadil Mahdi, Analysis of Zinc Oxide (ZnO) Thin nano Film Produced Using the Sol-Gel Method. Journal of Nanostructures, 2025. 15(2): p. 555-562.

[12] Noman, M.T., N. Amor, and M. Petru, Synthesis and applications of ZnO nanostructures (ZONSs): A review. Critical Reviews in Solid State and Materials Sciences, 2022. 47(2): p. 99-141.

[13] Iqbal, T., et al., Enhancing apple shelf life: A comparative analysis of photocatalytic activity in pure and manganese-doped ZnO nanoparticles. Materials Science in Semiconductor Processing, 2024. 173: p. 108152.

[14] Ozugurlu, E., Cd-doped ZnO nanoparticles: An experimental and first-principles DFT studies. Journal of Alloys and Compounds, 2021. 861: p. 158620.

[15] Zaman, Y., et al., Modified physical properties of Ni doped ZnO NPs as potential photocatalyst and antibacterial agents. Arabian Journal of Chemistry, 2023. 16(11): p. 105230.

[16] Kurtaran, S., Al doped ZnO thin films obtained by spray pyrolysis technique: Influence of different annealing time. Optical Materials, 2021. 114: p. 110908.

[17] Panchal, P., et al., Eco-friendly synthesis of Ag-doped ZnO/MgO as a potential photocatalyst for antimicrobial and dye degradation applications. Coordination Chemistry Reviews, 2023. 493: p. 215283.

[18] Khudiar, A.I. and A.M. Ofui, Effect of pulsed laser deposition on the physical properties of ZnO nanocrystalline gas sensors. Optical Materials, 2021. 115: p. 111010.

[19] Bai, N., et al., High-efficiency TiO2/ZnO nanocomposites photocatalysts by sol–gel and hydrothermal methods. Journal of Sol-Gel Science and Technology, 2021. 99(1): p. 92-100.

[20] Zhang, M., et al., UV-durable superhydrophobic ZnO/SiO2 nanorod arrays on an aluminum substrate using catalyst-free chemical vapor deposition and their corrosion performance. Applied Surface Science, 2023. 623: p. 157085.

[21] Rosli, N., M.M. Halim, and M.R. Hashim, Effect of CBD growth times on the ZnO microrods prepared on macroporous silicon. Applied Physics A, 2021. 127(9): p. 712.

[22] Ungula, J., et al., Investigation on the material properties of ZnO nanorods deposited on Ga-doped ZnO seeded glass substrate: Effects of CBD precursor concentration. Surface and Interface Analysis, 2022. 54(10): p. 1023-1031.

[23] Luwang, N.C., et al., Synthesis of ZnO nanostructure via CBD and solvothermal method using seed

technique. Journal of Sol-Gel Science and Technology, 2024. 112(3): p. 728-737.
[24] Abdulameera, Z.T., et al., Optical properties of ZnO nanorods and ZnO/CdZnS thin films. methods, 2022. 10: p. 12.
[25] Abdulrahman, A.F., N. Abd-Alghafour, and M.A. Almessiere, A high responsivity, fast response time of ZnO nanorods UV photodetector with annealing time process. Optical Materials, 2023. 141: p. 113869.